

Pulsed Laser Deposited Diode-Pumped 7.4 W Yb:Lu₂O₃ Planar Waveguide Laser

Tina L. Parsonage,* Stephen J. Beecher, Amol Choudhary, James A. Grant-Jacob, Ping Hua, Jacob I. Mackenzie, David P. Shepherd, and Robert W. Eason

Optoelectronics Research Centre, University of Southampton, Southampton, SO17 1BJ, UK

*t1p1g08@soton.ac.uk

Abstract: Fabrication, characterization, and laser performance of an Yb:Lu₂O₃ planar waveguide laser are reported. Pulsed laser deposition was employed to grow an 8 μm-thick Yb-doped lutetia waveguide on a YAG substrate. X-ray diffraction was used to determine the crystallinity, and spectroscopic characterization showed the absorption and emission cross-sections were indistinguishable from those reported for bulk material. When end-pumped by a diode-laser bar an output power of 7.4 W was achieved, limited by the available pump power, at a wavelength of 1033 nm and a slope efficiency of 38% with respect to the absorbed pump power.

© 2015 Optical Society of America

OCIS codes: (310.0310) Thin films, (230.7390) Waveguides, planar, (140.3380) Laser materials, (220.4610) Optical fabrication, (140.5680) Rare earth and transition metal solid-state lasers, (310.1860) Deposition and fabrication

References and links

1. H. J. Baker, J. R. Lee and D. R. Hall, "Self-imaging and high-beam-quality operation in multi-mode planar waveguide optical amplifiers," *Opt. Express*, **10**(6), 297–302 (2002).
2. C. T. A. Brown, C. L. Bonner, T. J. Warburton, D. P. Shepherd, A. C. Tropper and D. C. Hanna, "Thermally bonded planar waveguide lasers," *Appl. Phys. Lett.* **71**(9), 1139–1141 (1997).
3. J. I. Mackenzie, "An efficient high-power 946 nm Nd:YAG planar waveguide laser," *Appl. Phys. B*, **97**, 297–306 (2009).
4. R. Peters, C. Kränkel, K. Petermann, G. Huber, "Broadly tunable high-power Yb:Lu₂O₃ thin disk laser with 80% slope efficiency," *Opt. Express*, **15**(11), 7075–7082 (2007).
5. J. I. Mackenzie, "Dielectric Solid-State Planar Waveguide Lasers: A Review," *IEEE J. Sel. Top. Quant.*, **13**(3), 626–637 (2007).
6. T. Bhutta, J. I. Mackenzie, D. P. Shepherd and R. J. Beach, "Spatial dopant profiles for transverse-mode selection in multimode waveguides," *J. Opt. Soc. Am. B* **19**(7), 1539–1543 (2002).
7. T. C. May-Smith, J. Wang, J. I. Mackenzie, D. P. Shepherd and R. W. Eason, "Diode-pumped garnet crystal waveguide structures fabricated by pulsed laser deposition," *Conference on Lasers and Electro-Optics/Quantum Electronics and Laser Science Conference (CLEO/QELS)*, Long Beach, California (2006).
8. S. J. Beecher, T. L. Parsonage, J. I. Mackenzie, K. A. Sloyan, J. A. Grant-Jacob and R. W. Eason, "Diode-end-pumped 1.2 W Yb:Y₂O₃ planar waveguide laser," *Opt. Express*, **22**(18), 22056–22061 (2014).
9. T. C. May-Smith, A. C. Muir, M. S. B. Darby and R. W. Eason, "Design and performance of a ZnSe tetra-prism for homogenous substrate heating using a CO₂ laser for pulsed laser deposition experiments," *Appl. Opt.* **47**(11) 1767–1780 (2008).
10. "National Chemical Database Service," www.icsd.cds.rsc.org
11. J. W. Szela, K. A. Sloyan, T. L. Parsonage, J. I. Mackenzie, and R. W. Eason, "Laser operation of a Tm:Y₂O₃ planar waveguide," *Opt. Express*, **21**(10) 12460–12468 (2013).
12. C. Kränkel, "Rare-earth-doped sesquioxides for diode-pumped high-power Lasers in the 1-, 2-, and 3-μm spectral range," *IEEE J. Sel. Top. Quant.*, **21**(1), 1602013–1602013 (2015).

13. V. Peters, *Growth and spectroscopy of ytterbium-doped sesquioxides*, PhD thesis, University of Hamburg (2001).
 14. J. A. Caird, S. A. Payne, P. Randall Staver, A. J. Ramponi, L. L. Chase and W. F. Krupke, "Quantum electronic properties of the $\text{Na}_3\text{Ga}_2\text{Li}_3\text{F}_{12}:\text{Cr}^{3+}$ Laser," *IEEE J. Quantum Elect.*, **24**(6), 1077–1099 (1988).
-

1. Introduction

Planar waveguides doped with active ions have great potential in the development of high-power, diode-pumped solid-state lasers. The planar waveguide geometry has a high surface area to volume ratio that allows for effective thermal management of the gain medium, which is important for high-power lasers, and provides a system that is resilient to thermal lensing in the guided axis [1]. Most reports of high-power planar waveguide lasers to date have used the direct bonding fabrication technique [2, 3]. However, while high-quality waveguides can be achieved in this way it is a relatively slow and labour intensive process, therefore the use of planar waveguide lasers is somewhat limited in comparison to other laser geometries.

The sesquioxides Lu_2O_3 , Y_2O_3 , and Sc_2O_3 have been identified as promising host materials for high-power lasers due to their excellent thermomechanical properties [4]. These materials can be doped with ytterbium, an ion that is widely used for high-power solid-state lasers due to its low quantum defect. The combination of this dopant with these hosts has the potential to out-perform Yb:YAG lasers. However, these materials are not readily available commercially due to their high melting points, $\sim 2500^\circ\text{C}$ [4], which makes the growth of high-quality crystals, from the melt, particularly challenging.

Pulsed laser deposition (PLD) is a thin-film growth technique that allows crystalline films to be deposited on a substrate without the necessity to reach temperatures typically required for bulk growth from the melt. Material is repeatedly ablated from a target by incident laser pulses, causing a plume to be ejected towards a heated substrate, where thin-film growth occurs. This technique can be used to grow crystal layers on crystalline substrates with dissimilar refractive indices, allowing waveguides to be engineered to have a high numerical aperture (NA) compatible with high-power diode laser pumping. PLD can also be used to grow multilayer waveguides, forming double-clad structures that can be used to create a dopant profile that favours fundamental mode operation and therefore provides a near-diffraction-limited output in the guided direction [5, 6].

PLD of sesquioxides, doped with rare-earth ions, therefore lends itself to the manufacture of planar waveguide lasers. To date, only two examples of watt-class PLD-grown planar waveguide lasers have been reported, with the highest output being 4 W [7] from a garnet crystal waveguide and 1.2 W from an Yb: Y_2O_3 waveguide [8]. Here we report our recent progress towards power scaling these devices with a demonstration of 7.4 W from a diode-end-pumped Yb: Lu_2O_3 planar waveguide grown by PLD.

2. Fabrication

PLD was used to deposit an $\sim 8\ \mu\text{m}$ -thick Yb: Lu_2O_3 layer on a $10 \times 10 \times 1\ \text{mm}$ YAG $\langle 100 \rangle$ -oriented substrate. A KrF excimer laser operating at a wavelength of 248 nm, with pulse duration of 20 ns, and a repetition rate of 20 Hz was focused to produce a fluence of $\sim 1.3\ \text{J cm}^{-2}$ on the ceramic Yb: Lu_2O_3 target surface, in an oxygen atmosphere at a pressure of 2×10^{-2} mbar. The YAG substrate was heated to $\sim 900^\circ\text{C}$ from the rear by a $10.6\ \mu\text{m}$ CW CO_2 laser that undergoes a beam transformation through a ZnSe tetra-prism, such that the beam profile matches the square substrate surface and provides uniform heating [9]. An interfacial layer of $\sim 2\ \text{nm}$ Yb: Lu_2O_3 was deposited and annealed at $> 1000^\circ\text{C}$ for 5 hours prior to the main deposition to promote subsequent epitaxial growth at the YAG- Lu_2O_3 interface.

3. Sample characterization

The sample was analysed with X-ray diffraction (XRD) to characterise the crystallography, a surface profiler (KLA Tencor P-16) to measure the film thickness and an optical interferometric microscope to determine the surface morphology. Following initial characterisation of the deposited material, the sample was end-polished such that the opposing facets were plane and parallel, resulting in a waveguide length of ~ 8 mm.

For Yb:Lu₂O₃ growth on $\langle 100 \rangle$ -oriented YAG, the XRD analysis, performed using a Bruker D2 Phaser Diffractometer, contains sharp peaks, as shown in Fig. 1(a), indicating highly crystalline material. However, the Yb:Lu₂O₃ grows preferentially in the $\langle 111 \rangle$ orientation on the YAG $\langle 100 \rangle$ substrate due to lattice matching considerations. This is illustrated by the (222) and (444) peaks detected for the Lu₂O₃ overlapping the (400) and (800) peaks of YAG in the XRD spectra, making them practically indistinguishable. This is in agreement with spectra obtained from the crystal database [10] that has been used to identify the peaks present in Fig. 1(a), along with PDXL2 Version 2.1.3.4, Rigaku Corporation (2007-2013) software. Looking at the first 5 results on the crystal database for Lu₂O₃ (Ia-3 space group) and YAG, the (222) Lu₂O₃ peak 2θ values range from 29.78° to 29.88° and the (400) YAG from 29.78° to 29.80° , while the peak in our data sits at 29.78° .

The sample thickness was measured to be $8 \mu\text{m}$, and the number of surface particulates was counted at five positions over the sample by an optical interferometric microscope and

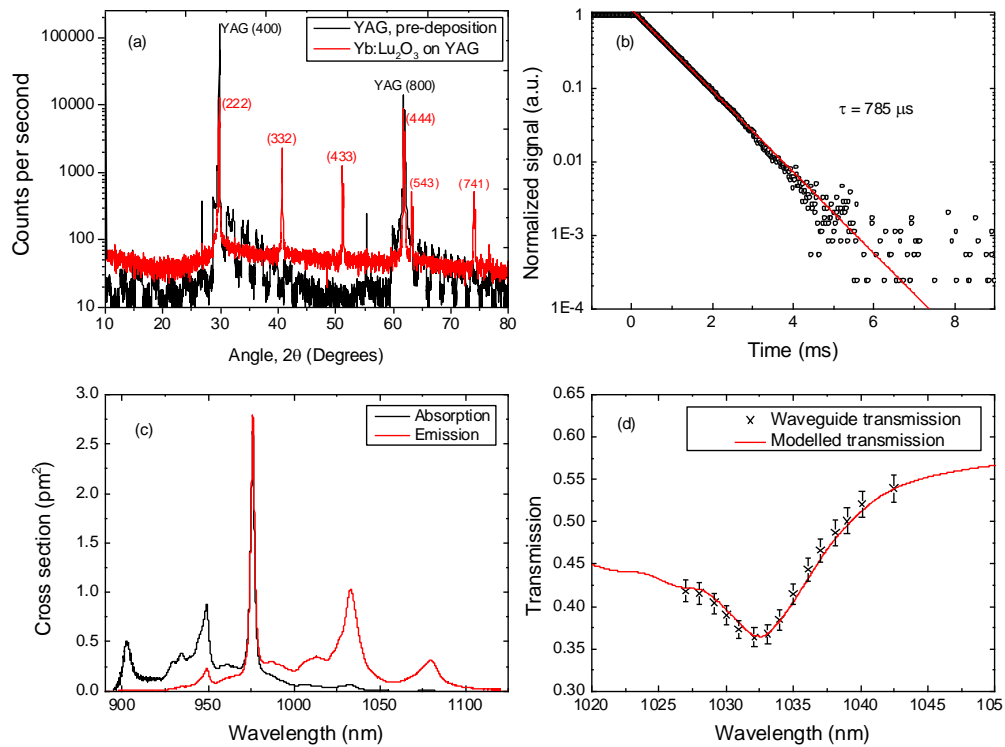


Fig. 1. (a) XRD spectrum of Yb:Lu₂O₃ grown on a YAG substrate in red, plotted with the XRD spectrum obtained from the bare YAG substrate prior to deposition in black. (b) Lifetime measurement taken for the Yb:Lu₂O₃ sample. (c) Absorption and emission cross-sections calculated from the fluorescence spectrum obtained from the Yb:Lu₂O₃ waveguide sample. (d) Transmission measurement of the sample as a means to obtaining the Yb concentration, with the experimentally measured points in black and modelled transmission in red.

associated software. Using the mean of these readings, the particulate density for this sample has been calculated to be approximately $1.5 \times 10^4 \text{ cm}^{-2}$ for particulates $>100 \text{ nm}$ and $2.2 \times 10^4 \text{ cm}^{-2}$ for particulates $>50 \text{ nm}$; these values are roughly comparable to those reported in [11] for particulates $>100 \text{ nm}$ and around a factor of 7x fewer for those $>50 \text{ nm}$.

To determine the emission characteristics, light from a broad-stripe diode laser operating close to the zero-phonon line, at 976 nm , was focussed into the $\text{Yb}:\text{Lu}_2\text{O}_3$ waveguide through one of the polished end facets. Fluorescence was captured from the top surface of the waveguide by a $62.5 \mu\text{m}$ core-diameter, 0.22 NA optical fiber positioned above the excited region of the waveguide. This collection geometry minimises the distance through doped material that fluorescence must travel before being collected, effectively reducing the spectrally dependent re-absorption loss of the Yb ions. The light captured by the fiber was measured using an optical spectrum analyser (ANDO AQ6317B), with a resolution of 0.2 nm . Due to an overlap of the fluorescence and pump spectra, pump light either scattered from the waveguide or not fully coupled into the guide can distort the measured spectra. To obtain a clean fluorescence spectrum two different measurements were made, with the pump laser wavelength-tuned, by adjusting the operation temperature and current, either side of the zero phonon line, at 959 nm and 981 nm . The two spectra had their pump-contaminated regions removed, were normalised to the 1033 nm emission peak and then averaged, resulting in a spectrum with negligible pump contamination and minimal influence from reabsorption losses. The fluorescence lifetime of the sample was measured under low excitation density, resulting in a measured lifetime of $785 \mu\text{s}$, as displayed in Fig. 1(b), slightly below the low concentration limit of the lifetime of $820 \mu\text{s}$ [4], evidencing a slight quenching.

An emission cross section for the sample was calculated using the Füchtbauer-Ladenburg equation assuming a unity quantum efficiency, a constant refractive index of 1.911 [12] and the reported low concentration lifetime of $820 \mu\text{s}$ [4]. The calculated emission cross section is shown in Fig. 1(c) and shows no significant differences from bulk crystals [13]. To calculate the absorption cross section the reciprocity technique was used in combination with McCumber analysis and the electronic Stark levels of the ground and excited state manifolds as reported by Peters [13].

To measure the Yb ion concentration in the sample two methods were used; energy dispersive X-ray analysis (EDX), which resulted in a value of $3.6 \pm 0.4 \text{ at. } \%$, and a method, as follows, that relies on the absorption of laser light from a tunable source by the Yb ions. Transmission measurements for the waveguide were taken for a range of wavelengths using a narrowband ($<0.1 \text{ nm}$ FWHM) tunable Yb: fiber laser. The laser was focussed to a spot of $7 \mu\text{m}$ diameter and coupled into the waveguide, and the output facet of the waveguide was imaged after magnification on to a narrow slit arranged to remove any potential contributions from light emerging from regions outside the waveguide core. Using this setup, the transmission through the system was measured for a range of wavelengths close to the 1033 nm absorption line. The transmission through the guide can be modelled well by assuming a broadband background insertion loss (IL) and a spectrally dependent loss due to absorption from the Yb^{3+} ions. Fig. 1(d) presents the measured transmissions and the expected transmission, modelled using Eq. (1), for a background IL of 2.35 dB and an Yb^{3+} density of $9.0 \times 10^{20} \text{ cm}^{-3}$.

$$\text{Transmission}(\lambda) = \frac{P_{\text{out}}}{P_{\text{in}}} = T_0 e^{-n_0 \sigma_{\text{abs}}(\lambda) l} \quad (1)$$

where T_0 is background, spectrally invariant transmission, n_0 is Yb ions per cm^3 , σ_{abs} is the absorption cross-section from Fig. 1 (c), but in cm^2 , and l is the length of the waveguide in cm. The background insertion loss includes a contribution of 0.9 dB from the two Fresnel reflections, 0.45 dB from each of the two uncoated facets, and a further 0.1 dB from residual reflections from AR coated coupling optics, thus resulting in an estimated upper limit on the

propagation loss of 1.35 dB, or 1.7 dB cm^{-1} . The Yb ion density of $9.0 (\pm 0.8) \times 10^{20} \text{ cm}^{-3}$ corresponds to a doping level of $3.2 \pm 0.3 \text{ at.}\%$ assuming a cation density identical to bulk, which is in agreement (within the quoted errors) with the value obtained by EDX.

4. Laser experiments

The waveguide was mounted on a water-cooled heatsink attached to a 5-axis translation stage and a pump input mirror (HT 950-990 nm, HR 1020-1100 nm) brought into close proximity to the pump input facet. The other facet was either used as the output mirror, relying on the Fresnel reflection of 9.8% from the Lu_2O_3 -air interface to provide feedback, or had an output coupling (OC) mirror brought into close proximity to the output facet. The Yb: Lu_2O_3 waveguide laser was pumped by a beam from a diode-laser bar operating around 976 nm that was focused by an acylindrical lens (AC1) to a diameter estimated to be $10 \mu\text{m}$ in the fast axis, at the input facet, and 1.2 mm in the slow axis, approximately half-way through the guide, with a system of cylindrical lenses as shown in Fig. 2. Cylindrical lenses C1 and C2 formed a telescope in the fast axis with a magnification of 6x and C3 loosely focused the beam in the slow axis.

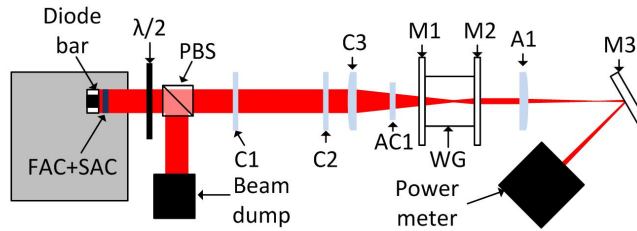


Fig. 2. Schematic of the optical system: FAC - fast axis collimator, SAC - slow axis collimator, PBS - polarising beam splitter, C1, C2 & C3 - cylindrical lenses, AC1 - acylindrical lens, M1 - pump input mirror, WG - waveguide, M2 - output coupler, A1 - aspheric lens, M3 - dichroic mirror.

To avoid shifts to the diode central wavelength when changing pump power the diode current and heatsink temperature were kept constant, and the pump power varied using a half-wave plate and polarising beam splitter. The output from the waveguide was collected with an aspheric lens ($f=18 \text{ mm}$, $\text{NA}=0.54$) and the laser light reflected by a dichroic mirror (HT 900-990 nm, HR 1020-1100 nm) onto a power meter. Pump light transmitted through the dichroic mirror, mainly from the extremes of the diode spectrum that have poor overlap with the Yb: Lu_2O_3 absorption spectrum, was recorded with another power meter, to assess the pump absorption efficiency. The laser output performance as a function of absorbed pump power for the different laser configurations trialled is presented in Fig. 3(a). The absorbed pump power plotted in Fig. 3(a) is an over estimate as not all of the incident pump light was coupled into the waveguide or captured by the collection lens. Therefore, it could not be accounted for in the determination of the absorption, derived from the transmitted pump power subtracted from the incident pump power.

The best performance obtained was from the laser setup using the Fresnel reflection of the output facet, which gave a maximum output power of 7.4 W and a slope efficiency of 38% with respect to estimated absorbed pump power. A Caird analysis [14] of the laser performance gives an estimate of the parasitic cavity loss to be 4.6 dB per round trip. The laser output wavelength was 1033 nm for all output couplers trialled, showing a high inversion density was required to reach threshold, consistent with moderate to high round-trip losses. The recorded spectrum, taken at maximum power operation, is shown in Fig. 3(b), showing no lasing at

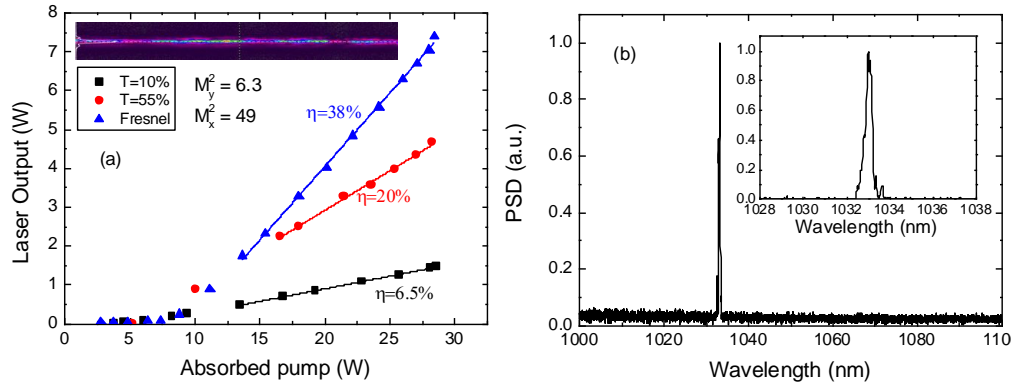


Fig. 3. (a) Laser output results for three different configurations, with the highest power measured at 7.4 W. The slope efficiency for each output coupler is displayed next to each slope in the corresponding colour. T = 10% OC in black, T = 55% OC in red, and lasing from Fresnel reflection at the output facet in blue. Inset image of the laser mode. (b) Yb:Lu₂O₃ laser spectrum at 7.4 W output power. Inset shows a zoomed-in view around the peak, from 1028 nm to 1038 nm.

other wavelengths and a zoomed-in view around 1033 nm. A waveguide of this thickness, 8 μm , operating at 1033 nm theoretically supports 9 modes, and second-moment beam-quality measurement established the laser output to be highly multimode with an M^2 of 6.3 in the guided axis and 49 in the unguided axis, at full power. The output mode of the laser, inset in Fig. 3(a), is consistent with the inhomogeneous sample structure previously seen in PLD-grown sesquioxides, as reported in [8] for Yb:Y₂O₃. This laser mode in the unguided axis is visibly improved compared to that seen in Y₂O₃ growth on <100>-oriented YAG, which we believe is due to the closer lattice match between the Lu₂O₃ and <100>-oriented YAG.

5. Conclusion

7.4 W of laser power has been obtained from a PLD-grown Yb:Lu₂O₃ waveguide on a <100>-oriented YAG substrate, with a slope efficiency of 38% with respect to absorbed pump power. There is no sign of thermal rollover, even at the highest pump powers used so far, despite minimal thermal management, which is a good indicator of the excellent thermal properties of these sesquioxide hosts. The output power obtained is currently limited by the available pump power, its launch conditions and absorption. In our setup, around 10 W of pump power was lost due to the spectral width of typical free-running diode bars exceeding that of the zero-phonon line of Yb:Lu₂O₃. Further improvements in the performance are expected by wavelength-narrowing the pump diode e.g. using a volume Bragg grating, polarisation multiplexing two diode bars together and by growing thicker waveguides capable of accepting the light from diode stacks or spatially multiplexed diode bars.

Acknowledgments

The authors acknowledge the support of the EPSRC through grant numbers EP/L021390/1, EP/N018281/1 and EP/J008052/1. Thanks to Dr Mark Light, School of Chemistry, University of Southampton, for assistance with XRD techniques and to Neil Sessions, Optoelectronics Research Centre, for assistance with EDX. Thanks to Callum Smith for use of his tunable fiber laser. The RDM data for this paper can be found at DOI: 10.5258/SOTON/381879.